A thermodynamic and N.M.R. study of the ribbon lyotropic mesophases. An investigation of the potassium palmitate/potassium laurate/water system

A. Raudino[a]; D. Grasso[a]; C. La Rosa[a]; G. Dipasquale[a]; G. Chidichimo[b]; A. Checchetti[b]

[a] Dipartimento di Scienze Chimiche, Universita' di Catania, Catania, Italy [b] Dipartimento di Chimica, Universita' della Calabria, Arcavacata di Rende, Cs, Italy

PLEASE SCROLL DOWN FOR ARTICLE

A thermodynamic and N.M.R. study of the ribbon lyotropic mesophases

An investigation of the potassium palmitate/potassium laurate/water system

by A. RAUDINO, D. GRASSO, C. LA ROSA and G. DIPASQUALE

Dipartimento di Scienze Chimiche, Universita' di Catania,
viale A. Doria 8-95125, Catania, Italy

G. CHIDICHIMO and A. CHECCHETTI

Dipartimento di Chimica, Universita' della Calabria,
Arcavacata di Rende (Cs) 87030, Italy

Lyotropic ternary mixtures of K-palmitate/K-laurate/water with different compositions have been investigated by ^{2}H N.M.R., differential scanning calorimetry and thermo-volumetric analysis. The transitions between rectangular ribbon-like aggregates and lamellar structures have been characterized and explained on the basis of a theoretical model. Our results suggest that for ternary systems containing a small amount of short chain lipids the ribbon structure is more stable at low temperature. Moreover, the rectangular shape is favoured both by the segregation of the short chain lipids at the curved edges of the ribbon and by a tighter packing of the hydrocarbon chains in the same region.

1. Introduction

It is well known from the literature that suitable ternary mixtures of lipids and water can form stable phases involving lipid aggregates of various shapes [1–3]. One of these is characterized by elongated ribbon shaped aggregates occuring in a relatively wide range of temperature and composition of the potassium palmitate, potassium laurate and water lyotropic mixtures [4–8]. The ribbon phase occurs between the L_β gel mesophase present at low temperature and the L_α liquid-crystalline phase at higher temperatures. The geometrical parameters of the ribbon phase have been defined by X-ray measurements [9, 10]. Nuclear magnetic resonance experiments performed on selectively deuteriated lipids or by dispersing the lipids in D_2O, showed that the potassium palmitate and laurate molecules are not randomly distributed throughout the lipid aggregate. In particular, the shorter potassium laurate molecules are more concentrated in the cylindrical edge of the ribbon, while the potassium palmitate molecules which have a longer chain lie mainly in the less curved lamellar part of the ribbon [4–8]. According to the criterion proposed by Israelachvili based on the critical packing parameter [11–12] such an inhomogeneous lipid distribution allows the formation of two coexisting regions with different curvatures.

In a recent paper [8] the authors have developed a simple thermodynamic model to predict the shape and stability of the ribbon aggregates as a function of different parameters, such as chemical structure, composition of the lipid mixture, interfacial tension and temperature. This model has been used to rationalize the ribbons-lamellae

or ribbon-cylinders phase transitions observed by ^{2}H N.M.R. measurements. In this paper we extend such a theoretical approach to calculate the variations of the specific heats associated with the polymorphic transitions involving ribbon phases. These predictions will be compared with differential scanning calorimetry and thermo-volumetric analysis data as well as with ^{2}H N.M.R. measurements on selected potassium palmitate, laurate watermixtures.

2. Theory
2.1. *Thermodynamic model*

To make this paper self-contained, we summarize briefly the basic ideas of the theory developed in [8]. The ribbons are made of flat and curved (lamellar or cylindrical region), as sketched in figure 1. In order to build up a thermodynamic model of the polymorphic phase transitions, it is useful to treat the flat and curved regions of the ribbon as two coexisting phases. The lipid components can distribute themselves between these two phases so minimizing the energy of the system. In contrast no exchange of matter between the aqueous solution and the lyotropic aggregate (which are truly different phases) has been allowed. This is a good approximation for systems with a low critical micellar concentration. The extent L of the lamellar region as well as the lipid composition of the two phases have been considered as variational parameters which can be obtained by minimizing the total energy of the system. This has been partitioned into five main contributions.
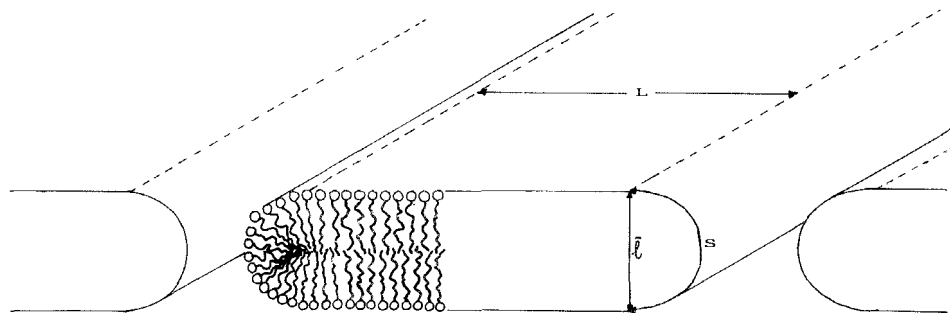
Figure 1.   Transverse section of a ribbon-like lipid assembly. S and L are the lengths of the cylindrical and lamellar regions, respectively.

(*1*) *Electrostatic energy*

If n_1^A and n_1^B are the number of long chain lipids present in phase A (lamellar) and B (cylindrical) and n_2^A and n_2^B be the corresponding quantities of the short chain component, then the electrostatic energy can be written as [8]

$$E_e = (n_1^A + n_2^A) \frac{C}{\bar{a}_A} + (n_1^B + n_2^A) \frac{C}{\bar{a}_B \left(1 + \dfrac{D}{R} \right)}. \tag{1}$$

Here $\bar{a}_A$ and $\bar{a}_B$ are the areas of the lipid head groups in the A and B regions, C and D are constants linked to the charge density at the lipid-water interface and R is the radius of curvature of the cylindrical region. Such an equation is an extension of that proposed by Israelachvili *et al.* in their theory of lipid assemblies [11]. Equation (1) can be simplified by noticing that: $n_1^A + n_2^A = n_A$, $n_1^B + n_2^B = n_B$ and $R = 1/2$

(see figure 1). The number of lipid molecules in regions A and B are related to the geometrical parameters L and S by the relationships

$$n_A = \frac{L}{L+S} N_T \quad n_B = \frac{S}{L+S} N_T, \tag{2}$$

where N_T is the total number of lipid molecules.

(2) Interfacial tension energy

According to [11], the interfacial tension energy is related to the lipid area a and to the lipid–water interfacial tension γ by $E_T \approx \gamma a$. This equation can be extended to the case of two coexisting mesophases [8] to give

$$E_T = (n_1^A + n_2^A) \gamma \bar{a}_A + (n_1^B + n_2^B) \gamma \bar{a}_B. \tag{3}$$

In writing equation (3) we have assumed that the interfacial tension does not change appreciably in the planar and curved regions.

(3) Chain energy

The interaction between the lipid chains (mainly due to van der Waals and short range repulsions) depends on the length of the hydrocarbon tails as well as on the shape of the lipid packing. Without loss of generality, we can assume that this energy is linearly related to the local concentration of the generic ith species in the jth phase. In the system studied we have two Lipid species (short and long chain molecules) and two regions (lamellar and cylindrical), consequently, the chain energy can be written as

$$E_c = -n_1^A g_1^A - n_2^A g_2^A - n_1^B g_1^B - n_2^b g_2^B, \tag{4}$$

where the coefficients g_i^j are related to the chains lengths of the lipids as will be discussed later.

(4) Mixing entropy

For a system formed by two components and one phase the entropy of mixing is [13]

$$S_{MIX} = -N_T k (X_a \log X_a + X_b \log X_b)$$

where, N_T is the total number of particles and X_a is the mole fraction of the ath component; clearly $X_b = 1 - X_a$. This equation can be generalized to consider the different entropic contributions arising from the two different regions of the ribbon aggregate to give

$$S_{MIX} = -k(n_1^A + n_2^A)(X_1 \log X_1^A + X_2^A \log X_2^A)$$
$$-k(n_1^B + n_2^B)(X_1^B \log X_1^B + X_2^B \log X_2^B), \tag{5}$$

where we have introduced the local mole fractions X_i^j, with $i = 1, 2$ and $j = A, B$. As shown in [8], the four local mole fractions X_i^j are not independent but are related through

$$X_1^A + X_2^A = 1; \quad X_1^B + X_2^B = 1; \tag{6a}$$

$$X_1^A = X_1 + \frac{S}{L}(X_1 - X_1^B), \tag{6b}$$

where the geometrical parameters L and S are defined in figure 1 and X_1 is the stoichiometric mole fraction of component 1.

(5) *Interaggregate interactions*

The appearance of rectangular phases introduces an additional repulsion between the curved edges belong to two adjacent ribbons (see figure 1). This energy is proportional to the number of charged lipid heads in the curved edges,

$$E_{INT} = (n_1^B + n_2^B)\,\xi, \tag{7}$$

where ξ is a parameter depending on the distance between the ribbons (i.e. on the lipid/water ratio) and on the salt concentration. ξ tends to zero for low concentrations of the lipid components (i.e. a large intermicellar distance) or high ionic strength (i.e. a screened coulombic repulsion). This energy term will be retained in the following formulas, however we believe that its contribution is extremely small when compared with the strong electrostatic and short range forces acting between the lipids belong to the same aggregate (see points 1 to 4).

Having defined the main energy contributions to the stability of the lyotropic structure, the coefficients determining the geometry and the lipid distribution within the aggregates can be obtained by minimizing the total energy with respect to the independent parameters. The number of such parameters can be reduced by recalling that n_1^A and n_1^B are related to n_A, n_B, X_1^A and X_1^B through the relationships (see equations (2))

$$n_1^A = n_A X_1^A = N_T \frac{L}{L+S} X_1^A, \quad n_1^B = n_B X_1^B = N_T \frac{S}{L+S} X_1^B; \tag{8}$$

Identical equations hold for n_2^A and n_2^B. Consequently, the only independent parameters are $\bar{a}_A$, $\bar{a}_B$, X_1^A and L. This set could be further reduced by assuming a constant volume V for the lipid aggregate and expressing the surface areas $\bar{a}_B$ as a function of $\bar{a}_A$ and V. This slightly different model has been investigated by us in [8].

Differentiating the total energy of the system with respect to the four independent parameters, equating the derivatives to zero and rearranging, we obtain a set of our non-linear algebraic equations

$$\frac{\partial E_{TOT}}{\partial \bar{a}_A} = \frac{L}{L+S}\left[-\frac{C}{\bar{a}_A^2} + \gamma\right] = 0, \tag{9a}$$

$$\frac{\partial E_{TOT}}{\partial \bar{a}_B} = \frac{S}{L+S}\left[-\frac{C}{\bar{a}_B^2\left(1+\dfrac{2D}{l}\right)} + \gamma\right] = 0, \tag{9b}$$

$$\frac{\partial E_{TOT}}{\partial X_1^A} = kT \log \frac{X_1^A X_2^B}{X_1^B X_2^A} + \Delta g_1 - \Delta g_2 = 0, \tag{9c}$$

$$\frac{\partial E_{TOT}}{\partial L} = \mathscr{A}(\bar{a}_A, \bar{a}_B) + kT(X_1^A \log X_1^A + X_2^A \log X_2^A \tag{9d}$$

$$- X_1^B \log X_1^B - X_2^B \log X_2^B)$$

$$+ kT \frac{L+S}{S}(X_1 - X_1^A) \log \frac{X_1^B}{X_2^B}$$

$$+ \Delta g_1 X_1 + \Delta g_2 X_2 + (\Delta g_2 - \Delta g_1)(X_1 - X_1^A) = 0,$$

where

$$\Delta g_1 \equiv - g_1^A + g_1^B; \quad \Delta G_2 \equiv - g_2^A + g_2^B,$$

and

$$\mathscr{A}(\bar{a}_A, \bar{a}_B) \equiv \frac{C}{\bar{a}_A} - \frac{C}{\bar{a}_B \left(1 + \dfrac{2D}{l} \right)} + \gamma(\bar{a}_A - \bar{a}_B) - \xi.$$

The analysis of the second derivatives shows that the extrema calculated from equation (9) are minima [8].

The system of equations (9) can be solved numerically. However in [8] some interesting limiting cases have been solved analytically. Simple expressions can be obtained when we consider systems containing a low concentration of short chain molecules mixed with a large amount of long chain species. Also the reverse situation leads to quite simple analytical solutions.

Knowledge of the set of parameters $S_1^0, S_2^0 \ldots S_M^0 \equiv \{S^0\}$ which minimize the energy of the system allows us to calculate the specific heat variations as a function of temperature. In fact, let $(E_{TOT})_{MIN} \equiv E_{TOT}(\{S^0\})$ and identifying $E_{TOT}(\{S^0\})$ with the true Gibbs energy G of the system, we have from the Gibbs–Helmholtz equation [13]

$$- \frac{H}{T^2} = \left[\frac{\partial}{\partial T} \left(\frac{G}{T} \right) \right]_p. \tag{10}$$

This equation can be simplifed by noticing that

$$\frac{\partial G}{\partial T} \equiv \frac{\partial}{\partial T} G(\{S^0(T)\}, T) = \left(\frac{\partial G}{\partial T} \right)_{\{S^0(T)\}} + \sum_{n=1}^{M} \left(\frac{\partial G}{\partial S_n^0} \frac{\partial S_n^0}{\partial T} \right) \tag{11}$$

but, according to equation (9) we have $\partial G/\partial S_n^0 = 0$ and so

$$\frac{\partial G}{\partial T} = \left(\frac{\partial G}{\partial T} \right)_{\{S^0(T)\}}. \tag{12}$$

Knowing H we may calculate the specific heat at constant pressure from

$$C_p = \left(\frac{\partial H}{\partial T} \right)_p. \tag{13}$$

Applying the previous formulas to the minimum energy structure of the ribbon calculated according to our model and making the reliable approximation $\partial \bar{a}_A / \partial T \approx \partial \bar{a}_B/\partial T$, we obtain, after some algebra,

$$C_p = \frac{S}{(L_0 + S)^2} (\alpha + \beta(X_1^A)_0) \frac{\partial L_0}{\partial T} + \frac{L_0}{L_0 + S} \beta \frac{\partial(X_1^A)_0}{\partial T}, \tag{14}$$

where $(X_1^A)_0$ and L_0 have been calculated by solving the system of equations (9). The parameters α and β are defined by

$$\begin{cases} \alpha \equiv 2\gamma(\bar{a}_A - \bar{a}_B) - \xi + \Delta g_2, & (15\,a) \\ \beta \equiv \Delta g_1 - \Delta g_2. & (15\,b) \end{cases}$$

If we neglect the small term $2\gamma(\bar{a}_A - \bar{a}_B) - \xi$ it follows that $\alpha > 0$ and $\beta > 0$, because the long chain lipid molecule 1 lies more favourably in the lamellar mesophase A rather than in the cylindrical region B of the ribbon. The opposite holds for the short chain component 2. In order to apply equation (14) we need to know the temperature dependence of (X_1^A) and L_0. This can be done by using the formulas developed in [8]. In particular, since in the present paper we are investigating ternary systems containing a low concentration of short chain lipids, we expect quite large ribbons (i.e. $S/L_0 \ll 1$) in which the shorter lipids are concentrated in the curved edge (i.e. $(X_1^A)_0 \approx X_1$). In this limiting case we obtain [8]

$$L_0 \propto \left(\frac{X_1}{1 - X_1} T \right)^{1/2}, \tag{16 a}$$

$$(X_1^B)_0 \propto \frac{X_1}{1 - X_1} \exp\left(\frac{\beta}{kT} \right). \tag{16 b}$$

Recalling equation (6 b) we can express $(X_1^A)_0$ as a function of $(X_1^B)_0$ and S/L_0. Inserting these results into equation (14) and neglecting higher order terms in S/L_0 we find the very simple equation

$$C_p \propto |T^{-3/2}| + O(|T^{-5/2}| \exp - |\beta|/kT). \tag{17}$$

The contribution to the specific heat calculated from this equation describes the effects arising from the lipid rearrangement within the lyotropic aggregates (i.e. the formation of the cylindrical edges and the segregation of the different lipids in the planar and curved regions of the ribbon). The experimental specific heats also contain contributions from the variations of the internal degrees of freedom of the lipid components. If we assume these terms to be constant in the lamellar and ribbon phases, C_p must decrease with temperature, caused by the transition from ribbons to lamellae. These qualitative predictions will be compared in the next section with our thermodynamic and N.M.R. data.

2.2. ^2H N.M.R. powder pattern

According to previous reports in the literature, the ribbon mesophase can be characterized through ^2H N.M.R. by measuring the deuterium quadrupole spectral patterns in samples where the aggregates are not uniformly aligned. The deuterons observed can be in some labelled positions of the lipids or can simply be those of D_2O molecules. Two parameters govern the shape of the ^2H N.M.R. spectra recorded from a particular nucleus in the lyotropic aggregates: the time averaged quadrupole constant ν_Q and the motionally induced asymmetry parameter η, which depends upon the diffusional motion of the molecules within the lyotropic aggregates (lipids) or around the aggregate (water). For spectra recorded from D_2O both these quantities can be connected to the probability, W, that the molecules interact with the flat part of the lipid assembly (the lamellar region A) through the relations [4, 5]

$$|\nu_Q^{RB}| = \frac{3W + 1}{4} |\nu_Q^L|, \tag{18 a}$$

$$\eta^{RB} = \frac{3(1 - W)}{3W + 1}, \quad \text{for} \quad \tfrac{1}{3} \leqslant W \leqslant 1, \tag{18 b}$$

$$|v_Q^{RB}| = \tfrac{1}{2}|v_Q^l|,$$

$$\left.\begin{array}{l} |v_Q^{RB}| = \tfrac{1}{2}|v_Q^l|, \\ \eta^{RB} = 3W, \end{array}\right\} \quad \text{for} \quad 0 \leqslant W \leqslant \tfrac{1}{3}.$$

$$(18\,c)$$

$$(18\,d)$$

The index RB denotes the ribbon mesophase. v_Q^l is the quadrupole coupling in a lamellar mesophase where the local order of the molecules is the same as that of the ribbon phase. Alternatively $|v_Q^l|$ can be expressed as $1/2\,|v_Q^C|$, where v_Q^C is the quadrupole coupling constant measured in a cylindrical mesophase. When the ribbon undergoes a phase transition to a hexagonal (H_α) or lamellar mesophase (L_α), v_Q^l and v_Q^C can be measured directly. Obviously, the use of such measured values of v_Q^l and v_Q^C is always based on the hypothesis that the local molecular order is unaffected by the RB $\rightarrow L_\alpha$ and RB $\rightarrow L_\alpha$ and RB $\rightarrow H_\alpha$ transitions and by the corresponding temperature variations. For water molecules, which can only diffuse around the lyotropic aggregates, the probability, W, can be taken as $L/(L + S)$.

It is then possible to obtain the shape of the ribbons and to identify the possible phase transitions to the hexagonal or lamellar mesophases by measuring v_Q^{RB} and η^{RB} and by following the evolution of such parameters as a function of temperature, as we now illustrate.
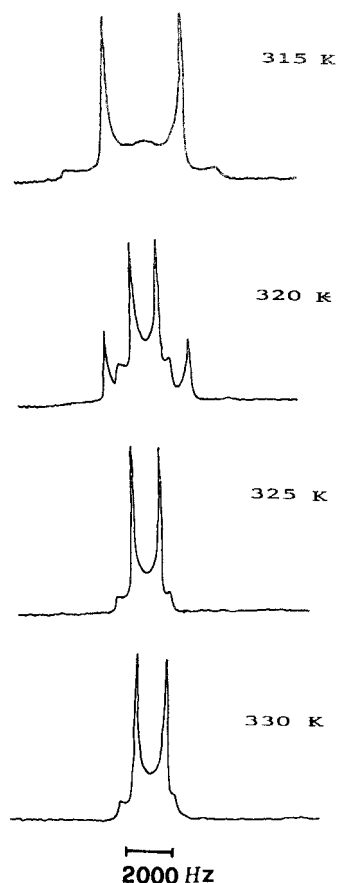
Figure 2. Deuterium N.M.R. spectral profiles recorded from ^2H_2O in a sample containing 68 percent potassium palmitate and 32 per cent of ^2H_2O.
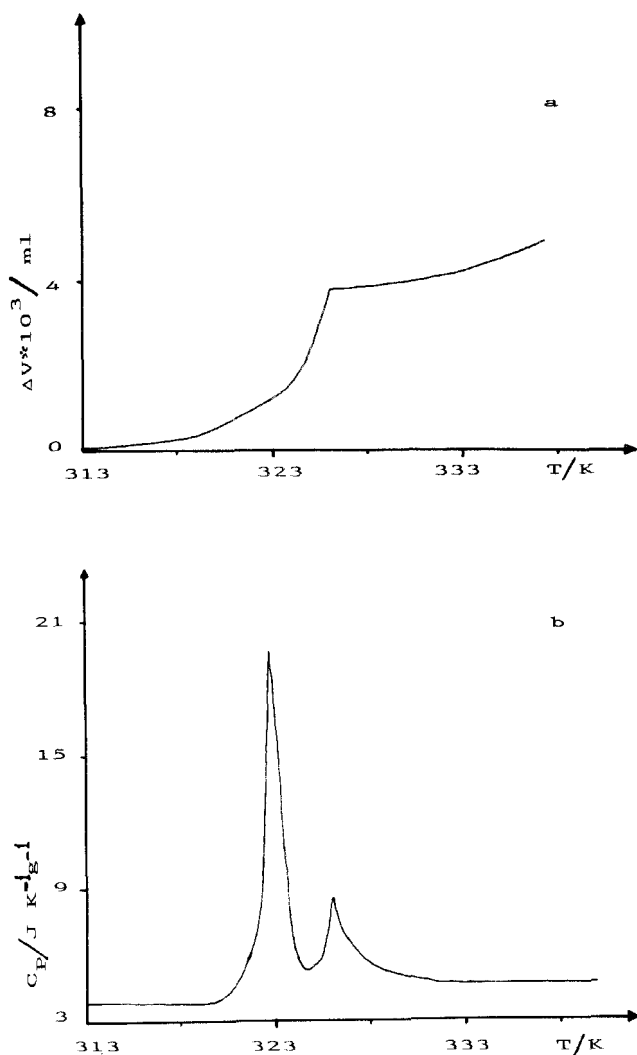
A. Raudino *et al.*

Figure 3. TVA (*a*) and DSC (*b*) curves for a sample containing 68 per cent of potassium palmitate and 32 per cent of ^2H_2O.

3. Experimental

The carboxylate salts have been prepared by treating the corresponding commercially available carboxylic acids with alcoholic potassium hydroxide. Compounds of satisfactory purity have been obtained by recrystalization from ethanol solutions. The samples were prepared by mixing the components in glass tubes sealed under a nitrogen atmosphere. Homogenization of the mixtures was achieved by alternatly centrifuging and heating the samples.

Measurements of the ^2H N.M.R. spectra were performed with a Bruker WM-300 spectrometer operating at 46 MHz. A mettler TC 10A processor equipped with a DSC 20 measuring cell was used for the calorimetric measurements after calibration for temperature and enthalpy using lauric, capric and myristic acids as standards. The range investigated was 30–60°C and the thermograms were recorded both in heating
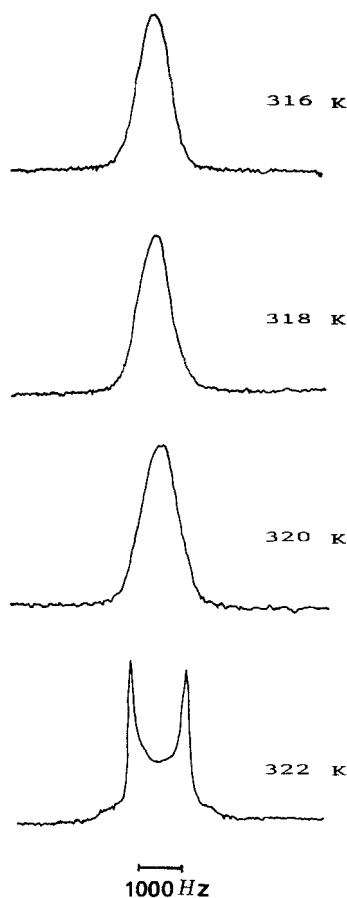
Figure 4. Deuterium N.M.R. spectral profiles recorded from ^2H_2O in a sample containing 61 per cent of potassium palmitate, 7 per cent of potassium laurate and 32 percent of ^2H_2O.

and cooling modes. The same processor equipped with a TMA 40 thermomechanical analyser was used to obtain measurements of the volume variation as a function of temperature at constant pressure. A quartz cylinder with a tight but freely movable piston was used as the sample holder; the movement of the piston was measured as a length change of the sample. The scan rates were 2°C/min for DSC and 1°C/min for TVA measurements, further details have been reported elsewhere [14].

4. Results and discussion

In order to have a comparison with the $L_\beta \rightarrow L_\alpha$ transition normally observed in two component systems, a sample containing 68 per cent of potassium palmitate and 32 per cent ^2H_2O was investigated. The ^2H N.M.R. spectra obtained from ^2H_2O is reported in figure 2 and clearly show a first order phase transition between the more ordered L_β phase ($v_Q = 4\cdot4\,kHz$) to the less ordered L_α phase ($v_Q = 1\cdot7\,kHz$). The transition evolves through a biphasic region near 320 K. On the other hand, the DSC curves (figure 3(b)) show two transitions in the same temperature range. The first peak can be attributed to the melting of the hydrocarbon chains whereas the second is probably related to water reorganization. To support this hypothesis we recall that
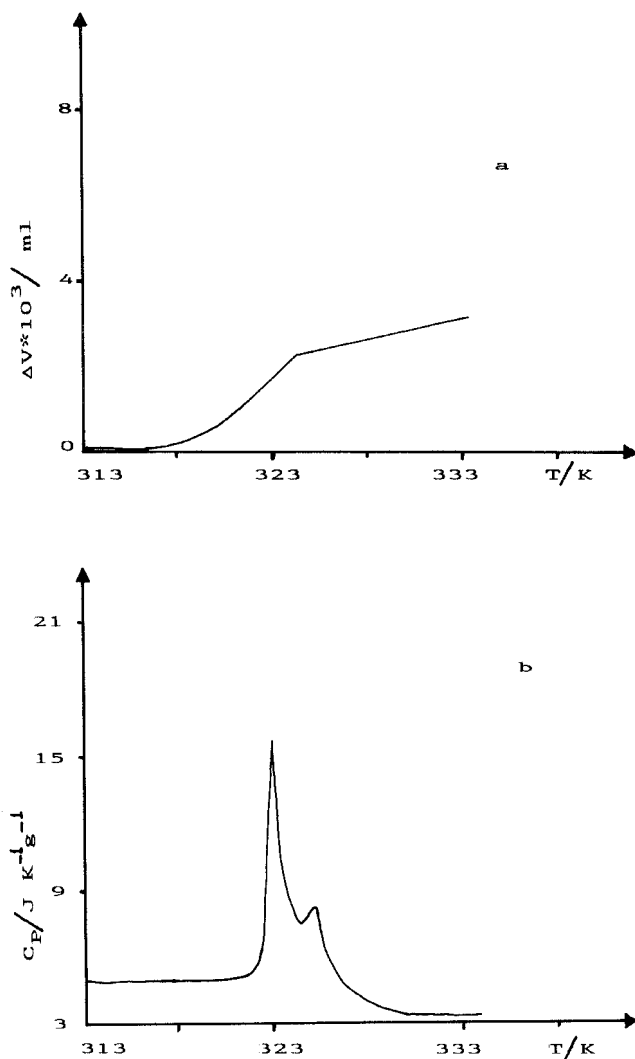
Figure 5.   TVA (a) and DSC (b) curves for a sample containing 61 percent of potassium
palmitate, 7 percent of potassium laurate and 32 percent of ^2H_2O.

only one peak has been observed in anhydrous potassium soaps [15]. The TVA curve
(see figure 3 (a)) shows a sharp transition in the same region. The large increase in
volume during the melting of the lipid chains has been observed in different classes
of phospholipids [16, 17]. When the behaviour of the ternary system containing 61 per
cent potassium palmitate, 7 per cent of potassium laurate and 32 per cent of ^2H_2O is
taken into account, the ^2H N.M.R. data show a transition at around 320 K (see figure 4).
On the basis of the results obtained in similar systems by X-rays [9, 10] and ^2H N.M.R.
profiles recorded from selectively deuteriated lipids [4–8], the ^2H_2O N.M.R. spectra
recorded between 313 and 320 K must be regarded as very asymmetric powder
patterns caused by the presence of a ribbon-like phase. On the other hand, the
spectrum at 322 K has the typical profile of the lamellar uniaxial mesophase.

The specific heat variations confirm these results. In fact, while for the binary
systems C_p is almost constant before and after the $L_\beta \rightarrow L_\alpha$ transition (apart from the
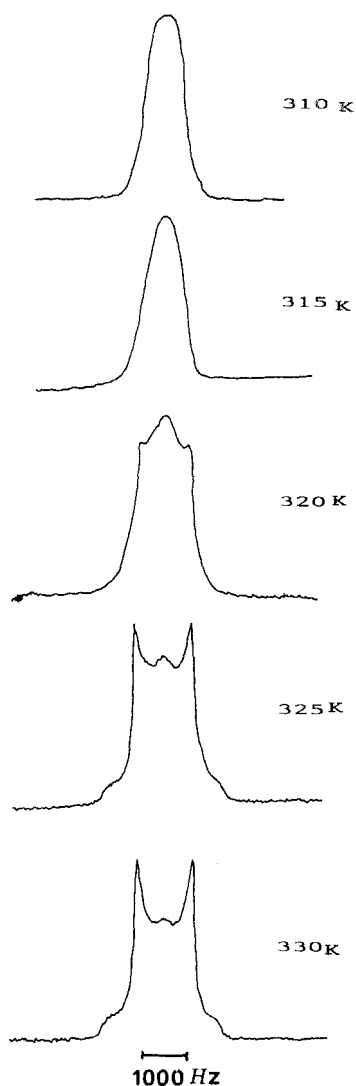
310 K

315 K

320 K

325 K

330 K

1000 *Hz*

Figure 6. Deuterium N.M.R. spectral profiles recorded from ^2H_2O in a sample containing 47 per cent of potassium palmitate, 21 per cent of potassium laurate and 32 per cent of ^2H_2O.

very slight increase of the base line common to many substances), when the ternary systems are taken into account the behaviour is reversed. As we can see from figure 5 (*b*), C_p is higher at low temperatures, then it decreased rapidly towards a constant value on raising the temperature. Furthermore, the two peak structure charactristic of binary systems is still present but its intensity is lower. These results agree well with our theoretical mode, which for a ternary lyotropic system containing a small amount of short chain species, predicts: (i) the ribbon phase is more stable than the lamellar at low temperatures; and (ii) the specific heat decreases on passing from the ribbon to the L_α phase.

The behaviour of the molar volume with the temperature adds new information concerning the structure of these lyotropic aggregates. In fact, the volume variation
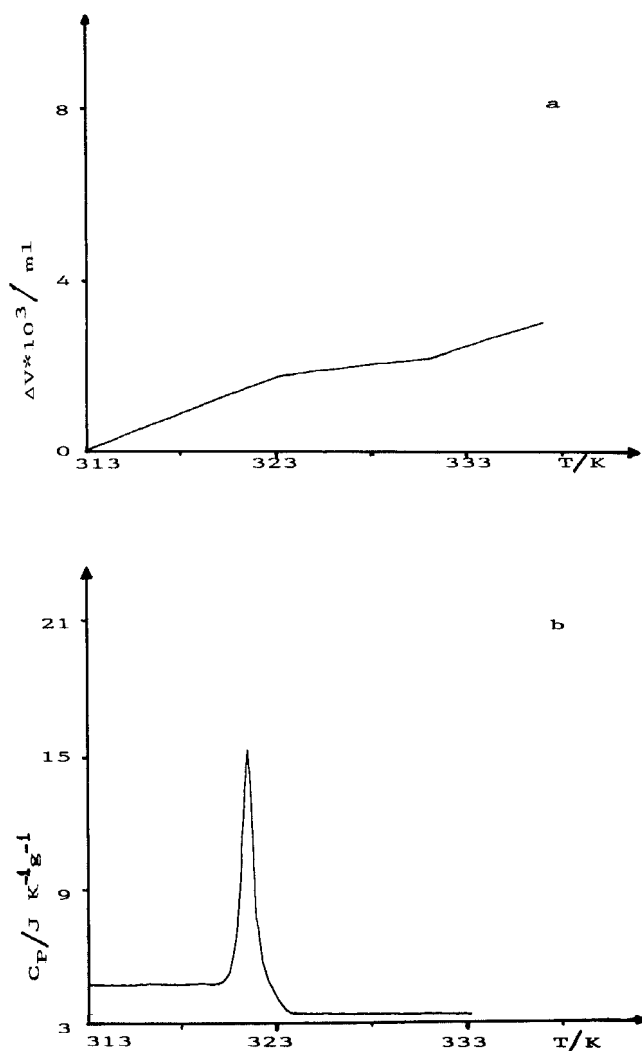
Figure 7. TVA (*a*) and DSC (*b*) curves for a sample containing 47 percent of potassium polmitate, 21 percent of potassium laurate and 32 percent of ^2H_2O.

of ternary systems do not exhibit the sharp discontinuity present in the binary systems (see figures 3 (*a*)) and 5 (*a*), suggesting that the order of the lipid chains in the ribbon phase should be inbetween that of the L_β and L_α phases. This is supported by previous ^2H N.M.R. spectra recorded from selectively deuteriated lipids which showed that the terminal methyl group of the lipid chains has a greater order in the curved region of the ribbon with respect to the L_α phase [6]. A further increase in the short chain lipid component leads to a destabilization of the lamellar structure. Consequently, at higher temperatures L_α can coexist with other structures having curved edges, as we can see from the ^2H N.M.R. profiles shown in figure 6. Moreover, the presence of two coexisting phases should lead to smoother variations in the TVA and DSC curves (see figure 7). The investigation of other lyotropic ternary mixtures containing the same amount of water but with other liquid compositions, did not alter these qualitative results and so is not reported here.

5. Concluding remarks

The results of the present paper are twofold. (*a*) The thermodynamic measurements and the theoretical model confirm many of the previous conclusions on ribbon stability, its evolution with temperature and lipid segregation in the different regions of the lyotropic aggregated based on N.M.R. and X-ray data (*b*) The thermodynamic data suggest that the RB $\rightarrow L_\alpha$ transition is favoured by decreasing the order parameter of the lipid chains as we can see from the presence of a sharp peak in the DSC curves of ternary systems. The same transition leads to a discontinuity in the TVA curves. Since the melting of the lipid hydrocarbon chains in binary systems forming only lamellar aggregates takes place at the same temperature as the RB $\rightarrow L_\alpha$ transition we can conclude that the ribbon structure is stabilized not only by the segregation of the short chain lipid molecules in the cylindrical edges of the ribbon, but also by the more ordered packing of the hydrocarbon chains in the same region. A more thorough study of the ribbon $\rightarrow$ cylinder phase transition is in progress in our laboratories.

References

[1] HENDRIKX, Y., and CHARVOLIN, J., 1981, *J. Phys. Paris.*, **42**, 1427.
[2] HENDRIKX, Y., CHARVOLIN, J., and RAWISO, M., 1984, *J. Colloid Interface Sci.*, **100**, 597.
[3] ALPERINE, S., HENDRIKX, Y., and CHARVOLIN, J., 1985, *J. Phys. Lett.*, **46** L-27.
[4] CHIDICHIMO, G., VAZ, N. A. P., YANIV, Z., and DOANE, J. W., 1982, *Phys. Rev. Lett.*, **49**, 1950.
[5] CHIDICHIMO, G., GOLEMME, A., DOANE, J. W., and WESTERMANN, P. W., 1985, *J. chem. Phys.*, **82**, 536.
[6] CHIDICHIMO, G., COLEMME, A., and DOANE, J. W., 1985, *J. chem. Phys.*, **82**, 4369.
[7] CHIDICHIMO, G., GOLEMME, A., RANIERI, G. A., TERENZI, M., and DOANE, J. W., 1986, *Molec. Crystals liq. Crystals*, **132**, 275.
[8] CHIDICHIMO, G., RAUDINO, A., and IMBARDELLI, D., *Colloids Surf.* (to be published).
[9] BENIGNI, S., and SPIELBERG, N., 1987, *Molec. Crystals liq. Crystals*, **150**, 301.
[10] LIS, L. J., QUINN, P. J., and COLLINS, J. M., *Molec. Crystals liq. Crystals* (in the press).
[11] ISRAELACHVILI, J. N., MITCHELL, D. J., and NINHAM, B. W., 1976, *J. chem. Soc. Faraday Trans. II*, **72**, 1525.
[12] MITCHELL, D. J., and NINHAM, B. W., 1981, *J. chem. Soc. Faraday Trans II*, **77**, 601.
[13] GUGGENHEIM, E. A., 1952 *Thermodynamics* (North-Holland).
[14] GRASSO, D., 1987, *Liq. Crystals*, **2**, 557.
[15] GRANT, R. F., and DUNELL, B. A., 1961, *Can. J. Chem.*, **39**, 359.
[16] NAGLE, J. F., and WILKINSON, D. A., 1982, *Biochemistry*, **21**, 3817.
[17] TRISTAN-NAGLE, S., WIENER, M. C., YANG, C. P., and NAGLE, J. F., 1987, *Biochemistry*, **25**, 4288.